Available online at www.sciencedirect.com
ScienceDirect
Geochimica et Cosmochimica Acta 75 (2011) 3469–3485
Geochimica et Cosmochimica Acta
www.elsevier.com/locate/gca

Microbially mediated re-oxidation of sulfide during dissimilatory sulfate reduction by *Desulfobacter latus*

T. Eckert [a,b,*], B. Brunner [c], E.A. Edwards [d], U.G. Wortmann [b]

[a] School of Environmental Sciences, University of Guelph, Guelph, ON, Canada
[b] Geobiology Isotope Laboratory, Department of Geology, University of Toronto, Toronto, ON, Canada
[c] Max Planck Institute for Marine Microbiology, Bremen, Germany
[d] Department of Chemical Engineering and Applied Chemistry, University of Toronto, Toronto, ON, Canada

Received 25 February 2010; accepted in revised form 16 March 2011; available online 27 March 2011

Abstract

Enzymatic reactions during dissimilatory sulfate reduction (DSR) are often treated as unidirectional with respect to dissolved sulfide. However, quantitative models describing kinetic sulfur isotope fractionations during DSR consider the individual enzymatic reactions as reversible (Rees, 1973). Brunner and Bernasconi (2005) extended this line of thought, and suggested that as long as cell external sulfide (CES) concentrations are high enough, CES may diffuse back across the cytoplasmic cell membrane and may subsequently be re-oxidized to sulfate. Here, we test this hypothesis by measuring the time evolution of the δ^{34}S-sulfate signal during DSR in closed system experiments under different levels of sulfide stress (0–20 mM and 0–40 mM total dissolved sulfide). Our results show that the measured δ^{34}S-sulfate signal is markedly different in the latter case and that the observed sulfate S-isotope time-evolution is incompatible with a Rayleigh type fractionation model. In contrast, our results are consistent with a sulfate reduction and fractionation model that allows for a cell internal oxidation of dissolved sulfide by a sulfate reducer.

1. INTRODUCTION

Dissimilatory sulfate reduction (DSR) is the fundamental process that links the geochemical cycles of carbon, sulfur, oxygen, and phosphorous (e.g., Berner, 1970, 1984; Wortmann and Chernyavsky, 2007). Dissimilatory sulfate reduction proceeds through a series of enzymatic reduction steps (e.g., Harrison and Thode, 1958; Kemp and Thode, 1968; Postgate, 1984; Madigan, 2006) and the overall reaction can be written as

$$2[CH_2O] + SO_4^{2-} \rightarrow H_2S + 2HCO_3^-,$$
$$\Delta G^0 = -77 \text{ kJ mol}^{-1}(CH_2O) \quad (1)$$

(Jørgensen, 2006). This reaction is energetically favorable and typically considered to be unidirectional with respect to dissolved sulfide. In this study, we define the different sulfide species of the sulfide pool as follows: The "sulfide pool" is referred to as total dissolved sulfide, $[H_2S]_{tot}$, which is comprised of dissolved (undissociated) sulfide $[H_2S]_{aq}$, dissociated sulfide, $[HS^-]$ and $[S^{2-}]$. In the following we will use both "hydrogen sulfide" and "H_2S" to designate the total sulfide, and explicitly specify when we refer to a single sulfide species.

Dissimilatory sulfate reduction is accompanied by a kinetic isotope effect (Szabo et al., 1950; Thode et al., 1951), which enriches the electron acceptor (i.e., sulfate) in ^{34}S. This ^{34}S enrichment of sulfate expresses a cumulative effect of the isotope enrichments associated with the individual enzymatic reduction steps during DSR. It is generally assumed that the enzyme specific enrichment is constant, however, the expression of this intrinsic enrichment depends on the ratio of the backward to forward

* Corresponding author at: Geobiology Isotope Laboratory, Department of Geology, University of Toronto, Toronto, ON, Canada.
E-mail address: thomas.eckert@utoronto.ca (T. Eckert).

0016-7037/$ - see front matter © 2011 Elsevier Ltd. All rights reserved.
doi:10.1016/j.gca.2011.03.034

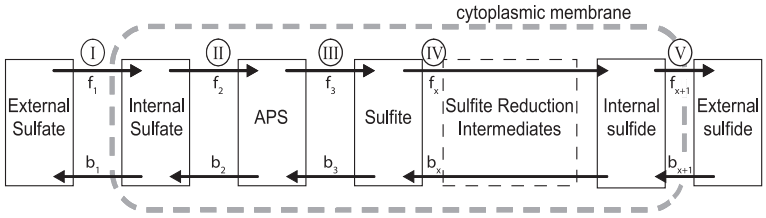

Fig. 1. Microbially mediated sulfate reduction proceeds through a series of individual enzymatic reduction steps, where each step can be associated with a fixed isotope fractionation factor. The magnitude of the total isotope effect is controlled by the upstream ratio of the backward and forward fluxes (Rees, 1973). See text for definitions of compartments, forward (f), and backward (b) fluxes (figure modified after Brunner and Bernasconi, 2005).

fluxes upstream of the respective reduction steps (see Fig: 1, and Rees, 1973). The backward to forward flux ratios can change as a response to changing physiological or environmental factors, for example, substrate availability and type, electron acceptor availability, temperature, or pH (e.g., Okabe et al., 1992; Ferenci, 1999; Knoblauch and Jørgensen, 1999; Habicht et al., 2005; Canfield et al., 2006; Moosa and Harrison, 2006). Consequently, the observed/net enrichment factor can vary and natural environments as well as experimental data show a large range of enrichment factors from −24 to −71‰ (e.g., Kaplan and Rittenberg, 1964; Canfield and Teske, 1996; Bolliger et al., 2001; Rudnicki et al., 2001; Wortmann et al., 2001; Werne et al., 2003; Canfield et al., 2010).

While the notion that the expression of the total isotope effect depends on the ratio between the forward and backward fluxes of the individual enzymatic steps has been used for decades (e.g., Harrison and Thode, 1958; Rees, 1973), only a few studies paid attention to the implied cell internal re-oxidation of reduced sulfur intermediates during sulfate reduction (e.g., Trudinger and Chambers, 1973; Brunner et al., 2005; Mangalo et al., 2007; Wortmann et al., 2007; Farquhar et al., 2008; Mangalo et al., 2008). Brunner and Bernasconi (2005) suggested that there is no reason to consider the transport of H_2S across the cytoplasmic cell membrane as a unidirectional step. They hypothesized that if the H_2S transport across the cytoplasmic cell membrane is bidirectional, step V in Fig. 1 would become a bottleneck that could result in the full expression of the upstream isotope effects. Such a scenario might explain the recent findings of enrichment factors with values of up to −72‰, which far exceeded the −47‰ predicted by the Rees-model (e.g., Rudnicki et al., 2001; Wortmann et al., 2001, 2007; Werne et al., 2003; Jørgensen et al., 2004; Canfield et al., 2010). Although microbial S-isotope fractionation is not solely a result of DSR and can also derive from disproportionation processes in the presence of oxidants (e.g., Canfield and Thamdrup, 1994; Cypionka et al., 1998), we focus here on DSR with a pure, sulfate reducing culture under strictly anaerobic conditions.

We test the hypothesis of a backward flux of undissociated sulfide, $[H_2S]_{aq}$, through the bacterial cell during DSR, which potentially allows the sulfate reducing organism to re-oxidize $[H_2S]_{aq}$ to sulfate, using stable sulfur isotope analysis. We propose that if such a backward flux through the bacterial cell exists, the backward flux should: (A) change the observed enrichment factor because it affects the ratios of the forward to backward fluxes, and (B) change the isotopic composition of the sulfate pool by adding isotopically light sulfate originating from the sulfide pool. In applying high/extreme sulfide concentrations, which can occur in natural environments (e.g., Wortmann et al., 2001; Lloyd et al., 2005), we further investigate the hypothesis whether these sulfide concentrations lead to high fractionations. We perform our experiments with a pure culture to distinguish physiological effects on the S-isotope fractionation from effects caused by a microbial community of a mixed culture. In the following, we compare the results of two independent batch culture experiments with *Desulfobacter latus* in: (A) a 'low sulfide' experiment (LSE) with $[H_2S]_{tot}$ concentrations between 0 and 20 mM, and (B) a 'high sulfide' experiment (HSE) with $[H_2S]_{tot}$ concentrations between 0 and 40 mM. We demonstrate that the HSE showed a distinctly different time-evolution of the δ^{34}S-sulfate signal compared to the low sulfide experiment.

2. METHODS

2.1. Organism and cultivation

The marine sulfate reducer *Desulfobacter latus* (DSMZ, #3381) was obtained from the Deutsche Sammlung von Mikroorganismen und Zellkulturen GmbH (DSMZ), Inhoffenstraße 7B, 38124 Braunschweig, Germany. *D. latus* is a complete oxidizer that solely grows on acetate as electron donor and carbon source, and sulfate as electron acceptor. *D. latus* lacks the ability to use sulfite or thiosulfate as electron acceptor (Widdel, 1987, 1988). This specialized growth behavior has two experimental advantages: First, it avoids S-isotope fractionation effects that could arise from the metabolism of more complex electron donors (Canfield, 2001). Second, a complete oxidizer is expected to produce larger S-isotope enrichments compared to incomplete oxidizers resulting in a more distinct δ^{34}S signal throughout the experiments (Detmers et al., 2001). Furthermore, *D. latus* is able to grow under sulfide stress conditions with $[H_2S]_{tot}$ concentrations exceeding 40 mM (Icgen and Harrison, 2006). With sulfate concentrations $\leqslant$30 mM, the culture can reach a doubling time of 21 h with a temperature optimum of 29–32 °C and a pH optimum between 7.0 and 7.3 (Widdel, 1987).

The initial *D. latus* inoculum from the DSMZ was transferred and cultivated in 120 mL serum bottles using 100 mL of the marine *Desulfobacterium* medium #383 (DSMZ)

with 20 mM of sulfate and $\geqslant$23 mM of acetate at pH = 7. Acetate was always present in excess to avoid a growth rate limiting effect of the substrate. Every four weeks, a 5% culture transfer was performed from the main culture into a fresh media bottle for maintenance. In contrast, prior to the LSE and HSE experiment, three culture transfers were performed in a fresh and slightly modified medium (see rationale below) as soon as all sulfate had been consumed (after approximately 6 days). Transferring the culture twice from the maintenance culture before growing the stock inoculum for an experiment ensured the most identical initial conditions for the LSE and HSE experiments. The timing of the transfer at the end of the growth phase further ensured that the inoculum was free of any remaining sulfate. The latter was chosen to minimize the interference of remaining sulfate when measuring $\delta^{34}S_{SO_4^{2-}}$ at time zero. The original DSMZ medium #383 was modified for the LSE and HSE as follows: Titanium(III)-citrate replaced the reductant $Na_2S \cdot 9H_2O$ (Zehnder and Wuhrmann, 1976; Jones and Pickard, 1980) as a precautionary measure to provide identical anaerobic conditions in all culture bottles at the beginning of the experiment, while avoiding any S-isotope interference of the reductant Na_2S with the experimental S-isotope results. In addition, a chelated trace element mixture with EDTA minimized any precipitation of trace metal sulfides (Widdel Bak, 1992). The medium was prepared anaerobically in a glovebox (Coy Laboratories, Michigan, with a N_2:CO_2:H_2 headspace 80:10:10% v/v) and 100 mL were dispensed into 120 mL serum bottles, sealed with blue butyl rubber stoppers (Bellco Glass, Inc.).

As mentioned above, a total of three culture transfers were performed in the modified medium before an experiment was started. Both the low sulfide and high sulfide batch culture experiment started with a 5 mL inoculum from a freshly grown stock culture using a self-refilling syringe as described by Kinoshita and Paynter (1988) and aseptic techniques. Monitoring the stock culture beforehand ensured that inoculation took place after all sulfate was consumed. The experiments were conducted at 23 °C in the dark. The LSE had an initial $[H_2S]_{tot}$ concentration of 0.3 mM as a result of the 5 mL inoculum, which was taken into account for all subsequent concentration and isotope calculations.

Two separate sets of batch culture experiments were conducted: the low sulfide experiment (LSE) with an initial $[H_2S]_{tot}$ concentration of 0.3 ± 0.1 mM ($\delta^{34}S_{H_2S}$: -4.6 ± 0.3‰ VCDT, resulting from the inoculum) and the high sulfide experiment, which was comprised of two feeding

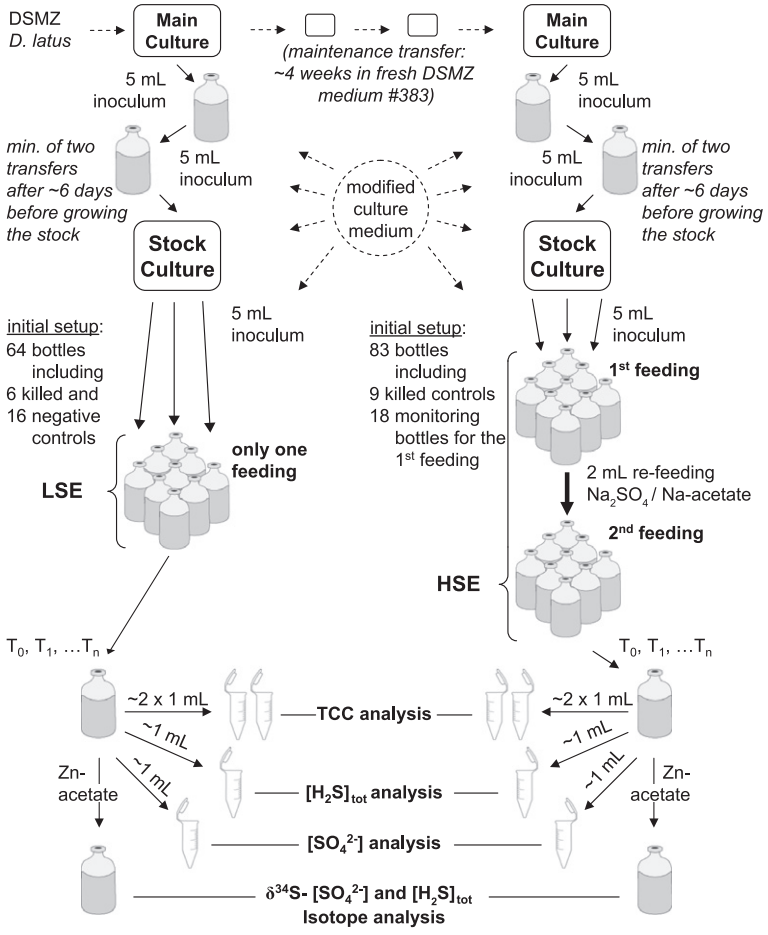

Fig. 2. Schematic experimental setup for both low sulfide (LSE) and high sulfide (HSE) experiments. Details about the individual stages can be found in the text (TCC = total cell counts).

cycles. The first feeding cycle of the high sulfide experiment was identical to the LSE and had an initial $[H_2S]_{tot}$ concentration of 0.2 ± 0.1 mM ($\delta^{34}S_{H_2S}$: -4.1 ± 0.3‰VCDT, resulting from the inoculum), whereas the second feeding cycle consequently had an initial $[H_2S]_{tot}$ concentration of 22.2 ± 0.5 mM ($\delta^{34}S_{H_2S}$: $+11.1 \pm 0.3$‰VCDT), see Fig. 2. Throughout our paper, the second feeding cycle of the high sulfide experiment is typically referred to as HSE and we clearly state when referring to the first feeding cycle of the high sulfide experiment. In the first feeding of the HSE, we used an isotopically heavier Na_2SO_4 ($\delta^{34}S_{SO_4^{2-}}$: $+11.0 \pm 0.3$‰ VCDT, provided courtesy of Saltex, LLC at Cedar Lake Facility, P.O. Box 1477, Seagraves, TX 79359, United States), whereas for the second feeding of the HSE, we used the same Na_2SO_4 ($\delta^{34}S_{SO_4^{2-}}$: -1.7 ± 0.3‰ VCDT) as for the LSE batch. The complete reduction of the Na_2SO_4, enriched in ^{34}S, to $[H_2S]_{tot}$ during the first feeding of the HSE enabled us to enhance the potential S-isotope effect of sulfide re-oxidation on the sulfate pool because the cell external sulfide (CES) had now a $\delta^{34}S$-value of +11.1‰ at the beginning of the second feeding of the HSE. Furthermore, the enriched Na_2SO_4 allowed us to test whether sulfate from the first feeding of the HSE was transferred to the second feeding stage. The presence of sulfate from the first feeding of the HSE could result in a significant change of the initial $\delta^{34}S_{SO_4^{2-}}$ value after re-feeding. However, after re-feeding, all of the six randomly sampled batch culture bottles at time $t(0)$ from the HSE had a uniform $\delta^{34}S_{SO_4^{2-}}$ isotope value, which was identical to the $\delta^{34}S_{SO_4^{2-}}$ value of the LSE.

2.2. Analytical procedures

Fig. 2 illustrates the experimental setup of both experiments. The LSE included 64 culture bottles with 6 killed and 16 negative controls whereas the HSE started off with 83 culture bottles including 9 killed controls. During the first feeding of the HSE, 18 culture bottles of the HSE were used to monitor the growth behavior. For each sacrificial culture bottle, duplicates of subsamples (up to 1 mL) were taken for total cell counts (TCC) and sulfate/sulfide analysis using aseptic techniques before preservation of the remaining medium in the serum bottle for isotope analysis. The latter was achieved by adding 3–5 mL of a concentrated or saturated Zn-acetate solution (20% w/v and 43% w/v, respectively) to the remaining medium in the culture bottle through the septum. The excess of Zn-acetate ($>10 \times [H_2S]_{tot}$) ceased any further sulfate reduction and preserved the $[H_2S]_{tot}$ as ZnS, including any H_2S from the headspace. The serum bottles were stored at 6 °C in a refrigerator. Triplicates of sacrificial culture bottles, and sextuplets at time $t(0)$ of the LSE and HSE, respectively, were sampled at each time point. Negative controls were sampled during the LSE: triplicates of negative controls at the start and finish, and a single sample during all but one of the sampling steps. Killed controls were sampled in triplicates at the start and finish of each experiment. During the HSE, triplicates of killed controls were sampled at the beginning of the experiment, after re-feeding and at the end of the experiment.

2.3. Bacterial cell numbers

During the LSE, TCC-samples were preserved in 1.5 mL microcentrifuge tubes with a 3.7% formaldehyde solution in 3.5% NaCl and stored refrigerated at 6 °C (Fry, 1988). Microcentrifuge tubes were weighed before and after sample addition to determine the accurate sample volume using a medium density of $\rho_{med} = 1.020 \pm 0.003$ g cm^{-3}. The preservation method of the TCC-samples was changed before the first and second feeding of the HSE because an increasing aggregation of cells in the preserved formaldehyde solution over time made an accurate counting of cells impossible. Thus, during the HSE, TCC-samples were transferred to 1.5 mL microcentrifuge tubes, immediately frozen in liquid nitrogen, and stored at −80 °C in a freezer. We did not find a significant difference in the total cell count numbers when testing both preservation techniques on a sample from the same culture. The frozen TCC-samples ensured reliable and reproducible cell counting (Hyun and Yang, 2003) after completion of the HSE experiment. The TCC-method was the preferred bacterial enumeration technique in this study because the medium was not completely clear and did not allow to use the optical density for enumeration.

For total cell counts analysis, an aliquot of 10 to max 750 µL from a preserved sample, depending on the anticipated number of cells, was transferred into a sterile 15 mL Falcon® tube and kept in the dark. The aliquot was topped up to 9 mL with a filter sterile 3.7% (with 3.5% NaCl) formaldehyde solution before 1 mL of a 10 µg L^{-1} DAPI solution was added to reach a final DAPI concentration of 1 µg mL^{-1}. The sample was incubated for 20 min at 37 °C and filtered on a 0.2 µm black Nucleopore® filter (Millipore/Whatman). The Nucleopore® filter was finally mounted on a slide in a paraffin sandwich with a cover slip for counting (Fry, 1988). Total cell numbers were determined with a Nikon Microphot-FXA epifluorescence microscope by counting a minimum of 400 cells or 200 fields of view per filter, whichever requirement was fulfilled first (standard deviation [SD] = 15%) (Fry, 1988). TCC with DAPI as the fluorescent stain do not distinguish between live/dead cells. Consequently, all following calculations are solely based on the total number of countable cells.

2.4. Growth yield

The growth yield Y is expressed as the ratio of biomass formed (grams dry weight) over the amount of electron donor (sulfate in grams or mole) consumed (Habicht et al., 2005):

$$Y = \frac{\text{grams dry weight of biomass formed}}{\text{grams or mole of sulfate}}. \quad (2)$$

To calculate the dry weight of the biomass, we assumed that the biovolume (BV) of *D. latus* has the shape of a prolate spheroid according to

$$\text{BV} = \frac{\pi}{6} \cdot W^2 \cdot L, \quad (3)$$

with W and L representing the width (2 μm) and length (4 μm) of the oval, elongated shape and dimensions of the bacterium (Widdel, 1987; Hadas et al., 1998). The estimated BV was 8.4×10^{-12} cm^3 cell^{-1} ([SD] = 25%, based on variations in the width and length of a bacterial cell). With the known BV, the dry weight fraction per cell was estimated at 2.7×10^{-12} g DW cell^{-1} ([SD] = 32%) assuming a buoyant cell density of 1.07 g cm^{-3} ([SD] = 2.8%) and a cell dry weight (DW) of 30% (w/w; [SD] = 20%; Bakken and Olsen, 1983; Habicht et al., 2005). Biomass concentrations were calculated from the total cell counts and the dry weight fraction per cell resulting in a propagated error of 35% [SD].

2.5. Cell specific sulfate reduction rate

The cell specific sulfate reduction rate (csSRR) was calculated as a function of substrate and biomass concentration according to the Monod model as described by Robinson and Tiedje (1983)

$$\frac{1}{X}\frac{dS}{dt} = -\frac{\mu_{max} \cdot S}{(K_s + S)} \cdot \frac{1}{Y}, \quad (4)$$

where dS/dt is the rate of electron donor consumption, S represents the electron donor concentration, X is the biomass concentration, μ_{max} is the maximum specific growth rate, K_s the half-saturation constant, and Y the growth yield. The csSRR was estimated by applying a non-linear regression of the integrated Monod Eq. (4) using the calculated yield from above with the statistical software JMP® by SAS. For the modeling, we used an average csSRR based on the results from both experiments (see below).

2.6. Sulfide and sulfate analysis

For each analysis, ⩽1 mL of medium was withdrawn from the serum bottle after vigorous shaking and preserved in pre-conditioned microcentrifuge tubes with up to 500 μL of a 20% w/v Zn-acetate solution, depending on the anticipated $[H_2S]_{tot}$ concentration. The sample volume was determined gravimetrically before the vials were stored in a closed container with a water saturated atmosphere at 6 °C to minimize any loss of H_2O through the centrifuge tube over time until analysis. Total dissolved sulfide was measured using an aliquot of up to 1 mL from the preserved ZnS sample after vigorous shaking following the methylene blue method of Cline (1969) and Fishman and Friedman (1989) on a Milton Roy, Spectronic 1001Plus spectrophotometer. Sulfide calibration standards were prepared in the same fashion as the samples by first preserving the standard in pre-conditioned microcentrifuge tubes with Zn-acetate before withdrawing an aliquot for the analysis. The latter ensured a comparable dilution treatment of the standards and samples during analysis.

For sulfate analysis, an aliquot from the supernatant of the ZnS preserved sample was first diluted and pre-filtered (0.2 μm) before being analyzed by ion chromatography on a Dionex LC-20 ion chromatograph (25 μL sample loop, with an AS-9/AG-9 column, GP-50 gradient pump (2 mL/min flow) and EG-40 conductivity detector using a 2 mM carbonate/0.75 mM bicarbonate eluent). Sulfate calibration standards were prepared in the same concentration range (0–42 mM) as the experimental samples to use identical sample preparation and dilution techniques for both calibration standards and samples. The analytical error of the sulfate analysis varied between 2% and 42% with a median of 6% based on an error propagation using single standard deviations (Funk et al., 2007). The large sulfate concentration error of 42% corresponded only to the lowest sulfate concentrations.

2.7. Isotope analysis of sulfide and sulfate

The serum bottles with the preserved ZnS were vigorously vortexed to homogenize the sample before transferring an aliquot into a falcon tube. The aliquot volume ranged from 2 to a maximum of ~100 mL, depending on the prevailing sulfide/sulfate content. Volumes above 50 mL were split into two falcon tubes. After centrifugation, the supernatant was separated from the pellet, filtered through a 0.45 μm filter, acidified with HCl to pH 2–4, and mixed with a 10 times excess of a 1 M $BaCl_2$ solution compared to sulfate, to precipitate $BaSO_4$ overnight (Mayer and Krouse, 2004). Samples with very low sulfate amounts were concentrated in a drying cabinet at 60 °C to reduce the volume of liquid and to enhance formation of $BaSO_4$. The precipitated $BaSO_4$ was washed 3 times with DI-water before being freeze dried for analysis.

The remaining pellet, which contained the ZnS, was treated with $AgNO_3$ to form Ag_2S, washed once with NH_4OH to remove the co-precipitated AgCl, and 3 times with DI-water before being freeze dried for analysis.

For the isotope measurements, we weighed 200 μg of $BaSO_4$ or Ag_2S into tin cups, after which vanadium pentoxide was added as a catalyst. Sulfur isotopes were subsequently measured on an EA/IRMS (elemental analyzer/isotope ratio mass spectrometry) system consisting of a Eurovector EA3000 elemental analyzer, coupled to a Thermo-Finnigan MAT 253 mass spectrometer in continuous flow mode via a Conflow III open split interface. Data are reported in the conventional δ-notation relative to the Vienna-Cañon Diabolo Troilite (VCDT) standard:

$$\delta^{34}S(‰) = \left(\frac{[^{34}S/^{32}S]_{sample}}{[^{34}S/^{32}S]_{VCDT}} - 1\right) \times 1000. \quad (5)$$

The system was calibrated for each run using triplicates of two of the following international standards for sulfide and sulfate: IAEA-S1 (−0.3‰ VCDT), IAEA-S2 (+22.67‰ VCDT), IAEA-S3 (−32.55‰ VCDT) and IAEA-SO5 (+0.49‰ VCDT), IAEA-SO6 (−34.05‰ VCDT), NBS-127 (+21.1‰ VCDT), respectively (CIAAW, 2007). The overall analytical error including sample preparation for the $\delta^{34}S$ analysis was ±0.3‰ ($n = 6$, Ag_2S) and ±0.3‰ ($n = 6$, $BaSO_4$) respectively with an instrument reproducibility of 0.1‰ ($n \geqslant 10$).

It should be noted that throughout our communication the enrichment factor ε is negative as a result of its definition in the Rayleigh equation according to Mariotti et al. (1981):

$$\frac{R_{s(t)}}{R_{s(0)}} = \frac{10^{-3}\delta_{s(t)} + 1}{10^{-3}\delta_{s(t=0)} + 1} = f^{(\alpha_{p_i,s}-1)}, \quad (6)$$

$$\varepsilon_{p_i,s}\ (‰) = (\alpha_{p_i,s} - 1) \cdot 1000, \quad (7)$$

with s being the index for the substrate $[SO_4^{2-}]$ and p_i being the index for the instantaneous product $[H_2S]_i$. $R_s(t)$ represents the $^{34}S/^{32}S$ ratio of the substrate at time t, f the remaining fraction of the substrate, $\delta_s(t)$ the measured $\delta^{34}S$ isotope value of the substrate at time t, and $\alpha_{p_i,s}$ and $\varepsilon_{p_i,s}$ the fractionation and enrichment factor, respectively.

3. MODEL DEVELOPMENT

The classical technique of describing fractionation processes inside a sulfate reducer is to use box models that express the sulfur fluxes and their associated fractionation between multiple cell internal pools along a reducing gradient, see Fig. 1 (e.g., Rees, 1973; Farquhar et al., 2003; Brunner and Bernasconi, 2005; Johnston et al., 2005, 2007; Hoek et al., 2006; Wortmann et al., 2007. We limit our model to the observable properties, namely the overall enrichment factor, the isotopic composition of the sulfate and sulfide pool, and the concentration of sulfate and total dissolved sulfide $[H_2S]_{tot}$. We thus use a simplified sulfate reduction and fractionation (SRF) model consisting of four fluxes from the two external sulfur pools – $[SO_4^{2-}]$ and $[H_2S]_{aq}$ – into and out of the bacterial cell (Fig. 3). We follow Brunner and Bernasconi (2005) and define the maximum enrichment factor for our SRF reflux model as $\varepsilon_{tot} = -70‰$. In contrast to ε_{tot}, the observed/apparent enrichment factor $\varepsilon_a(t)$ can be variable and depends on the ratio of the backward and forward fluxes $b_1(t)/f_1(t)$. We define $\varepsilon_a(t=0)$ as the initial enrichment factor that we use as a boundary condition for our model. The used rate unit in our model calculation is Mol cell^{-1} time^{-1} since the basis for our model is a single bacterial cell. As a result, the model allows us to use any scaling factor for the cell specific sulfate reduction rate (csSRR) and will still display the same model output under the assumption that the metabolic pathways and hence the fractionation factors of the individual pathways (Fig. 1) remain the same over time. In other words, our model is insensitive towards changes in the csSRR given the aforementioned assumptions.

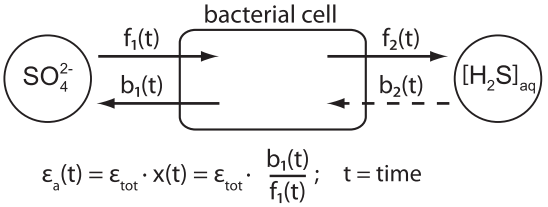

Fig. 3. Single step sulfate reduction and fractionation model to evaluate effects of undissociated sulfide ($[H_2S]_{aq}$) on $\delta^{34}S$ in the sulfate pool. The symbols $f_x(t)$ and $b_x(t)$ represent time dependent forward and backward fluxes, respectively. The apparent enrichment factor $\varepsilon_a(t)$ is defined by the quotient of b_x to f_x according to Rees (1973) with the maximum enrichment factor ε_{tot} representing the value of the highest possible enrichment of the organism. The ratio $x(t)$ between $b_1(t)$ and $f_1(t)$ determines the apparent enrichment factor based on ε_{tot}.

3.1. Model assumptions

To calculate the four fluxes that enter and leave the cells, $f_1(t)$, $b_1(t)$, $f_2(t)$ and $b_2(t)$, as defined in the previous section, a system of four equations was solved for each time step. The equation system is based on the initial concentrations and isotope values for $[SO_4^{2-}]$ and $[H_2S]_{tot}$,ε_{tot} and the csSRR. The equation system further depends on two additional parameters: the initial $\varepsilon_a(t=0)$ and the 1st order kinetic constant k_{re}, which defines the H_2S reflux as a function of the cell external dissolved hydrogen sulfide concentration $[H_2S]_{aq}$. We determine these parameters by fitting the model results against the experimental data. The four model equations are as follows:

1. The apparent enrichment factor $\varepsilon_a(t) \leqslant \varepsilon_{tot}$ depends on the two fluxes $b_1(t)$ and $f_1(t)$ to and from the sulfate pool across the bacterial cell membrane and the maximum enrichment factor ε_{tot} of the cell (Fig. 3). The apparent enrichment factor becomes variable with a changing flux ratio $b_1(t)/f_1(t)$ over time with $f_2(t)$ being the fractionating reduction step:
$$\varepsilon_a(t) = \varepsilon_{tot} \cdot \frac{b_1(t)}{f_1(t)}. \quad (8)$$
2. We assume that the cell internal sulfur pool is in steady state, i.e., the sum of the fluxes into the cell equals the sum of the fluxes out of the cell:
$$f_1(t) + b_2(t) = f_2(t) + b_1(t). \quad (9)$$
3. We further assume that the cell specific sulfate reduction rate csSRR equals the difference between fluxes into and out of the cell from both, the sulfate ($f_1(t)$ and $b_1(t)$) and sulfide pool ($f_2(t)$ and $b_2(t)$):
$$\text{csSRR} = f_2(t) - b_2(t) = f_1(t) - b_1(t). \quad (10)$$
4. The sulfide reflux $b_2(t)$ is proportional to the $[H_2S]_{aq}$ concentration, with k_{re} being a 1st order rate constant:
$$b_2 = k_{re} \cdot [H_2S]_{aq}. \quad (11)$$

The initial, apparent enrichment factor $\varepsilon_a(t=0)$ and k_{re} are determined by minimizing the root mean squared error (RMSE) of the modeled data compared to the measured data in a Rayleigh plot ($\ln(R_t/R_0)$ vs. $\ln f(SO_4^{2-})_t$) according to

$$\text{RMSE} = \sqrt{\frac{1}{n} \cdot \sum_{t=0}^{t=t_{end}} \left(\ln f(SO_4^{2-})_{t,mod} - \ln f(SO_4^{2-})_{t,exp}\right)^2}, \quad (12)$$

with $\ln f(SO_4^{2-})_{t,mod}$ being the model and $\ln f(SO_4^{2-})_{t,exp}$ the experimental result respectively for the remaining substrate fraction f, and n being the number of data points between time $t=0$ and the end of the experiment ($t = t_{end}$). If k_{re} is zero in the SRF model, consequently $\varepsilon_a(t)$ is constant throughout the sulfate reduction with $\varepsilon_a(t) = \varepsilon_a(t=0)$ and

the SRF model equals the classical Rayleigh type fractionation model (Mariotti et al., 1981). The latter represents the case, in which $\varepsilon_a(t)$ is constant throughout the experiment and the sulfate reduction process is uni-directional with respect to the $[H_2S]_{aq}$ flux, i.e., no $[H_2S]_{aq}$ reflux through the bacterial cell occurs as required for a Rayleigh type fractionation (Mariotti et al., 1981).

3.2. Initial conditions

The initial conditions for the SRF model are calculated from the initial $[SO_4^{2-}]$, $[H_2S]_{tot}$ concentrations, and $\delta^{34}S$-values assuming an average csSRR as well as the best-fit results for ε_0 and k_{re}. Initial conditions at time $t = 0$:

$$\begin{aligned} f_1(0) &= \tfrac{\text{csSRR}}{1-x(0)}, & f_2(0) &= \text{csSRR} + b_2(0), \\ b_1(0) &= \tfrac{x(0)\cdot\text{csSRR}}{1-x(0)}, & b_2(0) &= k_{re}\cdot[H_2S]_{aq}(0), \\ x(0) &= \tfrac{\varepsilon_0}{\varepsilon_{tot}}, & \varepsilon_{tot} &= -70‰. \end{aligned} \tag{13}$$

Starting from the initial model setup, the consecutive cell internal fluxes, $\varepsilon_a(t)$, and the total dissolved sulfide concentration $[H_2S]_{tot}$ at time t are derived as a function of the sulfate concentration $[SO_4^{2-}](t)$ with:

$$\begin{aligned} b_2(t) &= k_{re}\cdot[H_2S]_{aq}(t), & f_2(t) &= \text{csSRR} + b_2(t), \\ b_1(t) &= b_1(0) + b_2(t), & f_1(t) &= \text{csSRR} + b_1(t), \\ \varepsilon_a(t) &= \varepsilon_{tot}\cdot\tfrac{b_1(t)}{f_1(t)}. \end{aligned} \tag{14}$$

With the assumption that only $[H_2S]_{aq}$ is diffusing through the bacterial cell membrane (e.g., Cypionka, 1987, 1989), an intermediate step was necessary to determine the undissociated $[H_2S]_{aq}$ based on the existing pH and the 1st dissociation constant of the $[H_2S]_{aq}/[HS^-]$ system ($K_{a1} = 10^{-7.05}$; Lide, 2006), assuming that at a pH of 7 ± 0.3 the total dissolved $[H_2S]_{tot}$ can be approximated by $[H_2S]_{aq}$ and $[HS]^-$ according to:

$$K_{a1} = \frac{[HS]^-\cdot[H]^+}{[H_2S]_{aq}}, \tag{15}$$

$$[H_2S]_{tot}(t) \approx [H_2S]_{aq} + [HS]^-, \tag{16}$$

$$[H_2S]_{tot}(t) = [H_2S]_{tot}(t-1) + [SO_4^{2-}](t-1) - [SO_4^{2-}](t), \tag{17}$$

and

$$[H_2S]_{aq} = \frac{[H]^+}{K_{a1} + [H]^+}\cdot([H_2S]_{tot}(t-1) + [SO_4^{2-}](t-1) - [SO_4^{2-}](t)). \tag{18}$$

The evolution of the pH curve was estimated with the geochemical model PHREEQC-2 (Parkhurst and Appelo, 1999). Modeling of the pH trend was accomplished by using the initial medium composition as input and assuming a stochiometric consumption of sulfate and acetate over time according to the equation:

$$CH_3COO^- + SO_4^{2-} \rightarrow 2\ HCO_3^- + HS^-|,$$
$$\Delta G^{0\prime} = -57\ \text{kJ}. \tag{19}$$

The pH calculation took into account a headspace of max 20 mL in the culture bottles that allowed the formation of $[H_2S]_g$ in the gas phase. The results showed that $[H_2S]_g$ accounted for less than 1.7% of the total dissolved sulfide concentration ($[H_2S]_{tot}$), which was measured with an average uncertainty of 6% during the experiment. Since the uncertainty of the expected $[H_2S]_g$ concentration was more than 3-fold smaller than the uncertainty of the $[H_2S]_{tot}$, the measured concentration of $[H_2S]_{tot}$ was not corrected for $[H_2S]_g$ concentration in the head space.

Once the cell internal flow rates are characterized for a given time step, the change in the sulfur isotope composition of sulfate can be calculated using rate expressions for $[^{32}SO_4^{2-}]$ and $[^{34}SO_4^{2-}]$ similar to the stable isotope distribution model of Jørgensen (1979) as follows:

$$\begin{aligned} \frac{\Delta[^{32}SO_4^{2-}]}{\Delta t} &= \frac{\alpha\cdot[^{32}SO_4^{2-}]}{[SO_4^{2-}]+(\alpha-1)\cdot[^{32}SO_4^{2-}]}\cdot\text{csSRR}, \\ \frac{\Delta[^{34}SO_4^{2-}]}{\Delta t} &= \frac{[^{34}SO_4^{2-}]}{\alpha\cdot[SO_4^{2-}]-(\alpha-1)\cdot[^{34}SO_4^{2-}]}\cdot\text{csSRR}, \end{aligned} \tag{20}$$

where values in brackets denote concentrations in the bacterial cell, α is the fractionation factor and csSRR is the cell specific sulfate reduction rate.

4. RESULTS AND DISCUSSION

4.1. Bacterial growth

The cultures showed exponential growth trends during the LSE and all feedings of the HSE (Fig. 4). During the second feeding of the HSE, the doubling time increased by a factor of 3.6 compared to the LSE, whereas the doubling time of the first feeding of the HSE was comparable to the doubling time of the LSE (Fig. 4). However, the prolonged doubling time during the second feeding of the HSE had no significant influence on the yield Y when compared with the LSE (Fig. 5). Statistically, we cannot distinguish between the yield of the LSE and the yield of the HSE as a result of the propagated error associated with the TCC (Fig. 5). Although the HSE data in Fig. 5 suggest a trend towards a smaller yield compared to the LSE, this implied trend could simply be a result of the used TCC method, which does not discriminate between live/dead cells and thus potentially overestimates the active biomass during the second feeding of the HSE. Thus, in a first approximation we assume that the growth yields of both LSE and HSE are identical and estimate Y through a weighted linear regression based on the biomass and the sulfate concentration data from both experiments (Fig. 5). This approach is supported by results from Moosa and Harrison (2006), who observed no significant change in the growth yield during a continuous, mixed culture study with sulfate reducing bacteria (SRB) and calculated/measured $[H_2S]_{tot}$ concentrations of 46.8 mM and 37.1 mM, respectively. Nonetheless, the reduced doubling time, which corresponds to the maximum growth rate μ_{max} and therefore the csSRR, needs to be treated with caution and could hint at an increased maintenance energy requirement of the organism (Okabe et al., 1995). For a discussion of the potential effects of a reduced doubling time during the HSE on the isotopic signature compared to the LSE see below (Section 4.2 D).

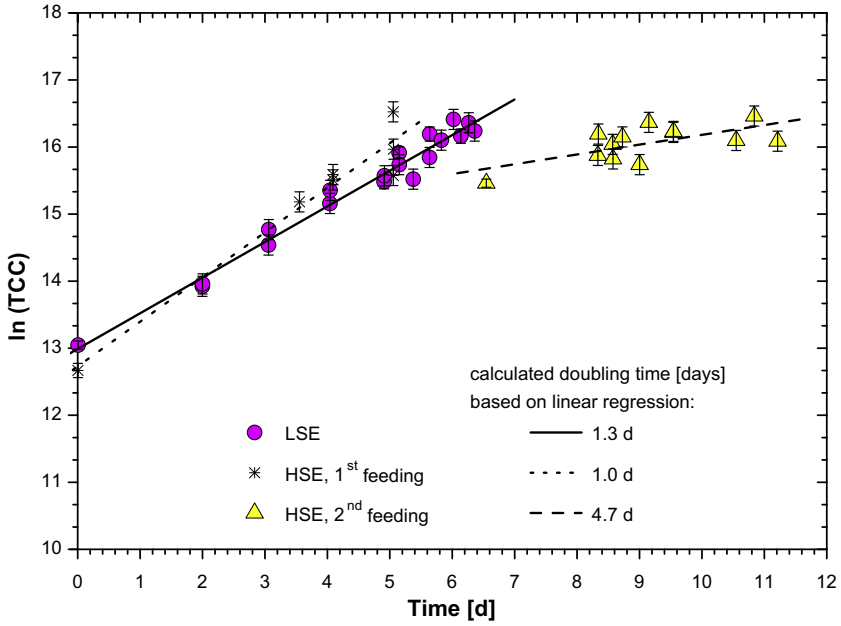

Fig. 4. Growth curves for the LSE and both feedings of the HSE based on total cell counts (TCC). The slope of the linear regression was used to calculate the doubling times. The figure shows the regression lines and final values of the calculated doubling times for the LSE (circles, solid line), the first feeding of the HSE (stars, dotted line), and the second feeding of the HSE (triangles, dashed line).

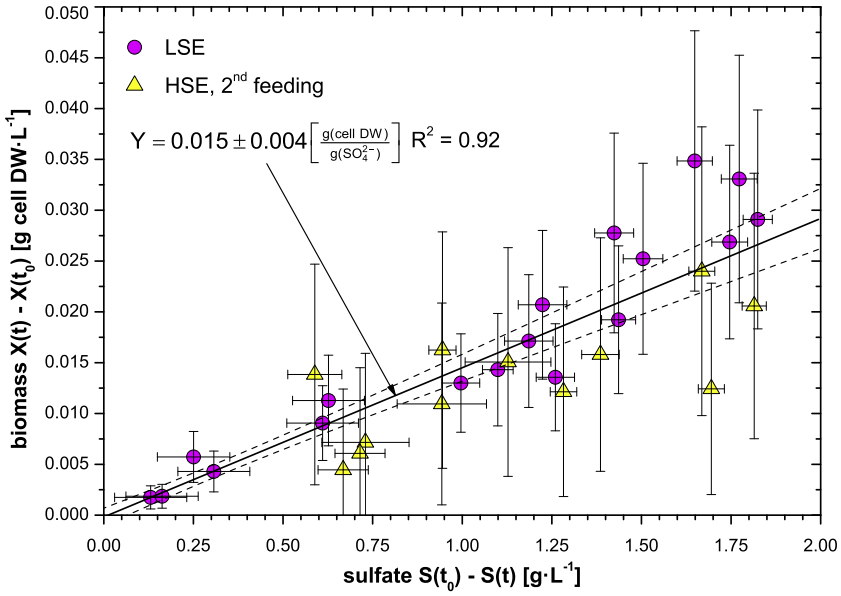

Fig. 5. Estimated growth yield (Y) based on a weighted linear regression through data from the LSE (circles) and second feeding of the HSE (triangles). Y represents the slope of the weighted regression (solid line), not forced through zero. Dashed lines represent the 95% confidence interval for the regression line and not the prediction limit for the measured data, which is much larger. Error bars are the result of an error propagation using single standard deviation.

4.2. Sulfur isotope fractionation

Fig. 6 shows the measured S-isotope compositions of SO_4^{2-} (circles and triangles) and H_2S (diamonds and squares) plotted versus the remaining substrate fraction f (SO_4^{2-}) for the LSE (circles and diamonds) and HSE (triangles and squares) experiments. Both data sets show the expected $\delta^{34}S_{SO_4^{2-}}$ trend towards heavier sulfate as the experiments progress. However, despite using the same experimental conditions except for the $[H_2S]_{tot}$ concentrations, the S-isotope data of sulfate (triangles) for the second feeding of the HSE show a significant offset towards heavier $\delta^{34}S_{SO_4^{2-}}$ values compared to the $\delta^{34}S_{SO_4^{2-}}$ data of the LSE (circles) for our pure culture setup with *D. latus*. The $\delta^{34}S$

differences of the initial $[H_2S]_{tot}$ between HSE (squares) and LSE (diamonds) are the result of using a Na_2SO_4, enriched in ^{34}S, for the first feeding of the HSE, followed by a re-feeding with the same Na_2SO_4 as in the LSE (see Section 2).

As can be seen from Fig. 6, the initial conditions are the same for the LSE and the second feeding of the HSE with respect to sulfate. However, if we try to fit the $\delta^{34}S_{SO_4^{2-}}$ data with a Rayleigh type fractionation model in log/log space,

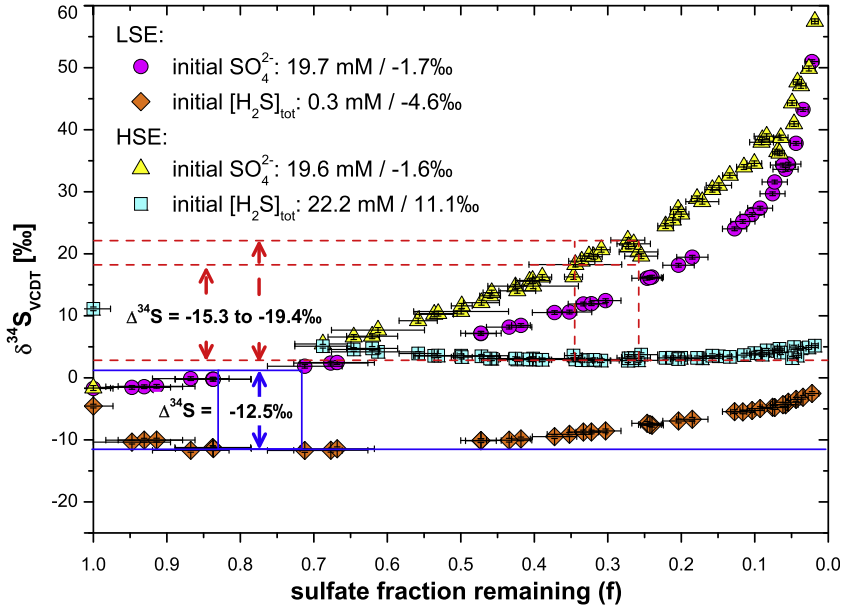

Fig. 6. Sulfur isotope fractionation trends of $\delta^{34}S_{SO_4^{2-}}$ and $\delta^{34}S_{H_2S}$ during batch culture experiments with *D. latus*. Circles (SO_4^{2-}) and diamonds (H_2S) represent the low sulfide experiment (LSE), 0.3–20 mM $[H_2S]_{tot}$, whereas triangles (SO_4^{2-}) and squares (H_2S) depict the second feeding of the high sulfide experiment (HSE), 22–40 mM $[H_2S]_{tot}$. The more enriched $^{34}S_{H_2S}$ starting point of +11.1‰ for the HSE compared to the −1.6‰ of $\delta^{34}S_{SO_4^{2-}}$ in the LSE was generated by using Na_2SO_4, enriched in ^{34}S, for the first feeding cycle of the HSE. The solid box and arrow as well as the dashed box and arrows indicate the estimated enrichment factors as $\Delta^{34}S$ ($\delta^{34}S_{H_2S} - \delta^{34}S_{SO_4^{2-}}$) of the instantaneous product in the LSE and HSE, respectively (for more information see text).

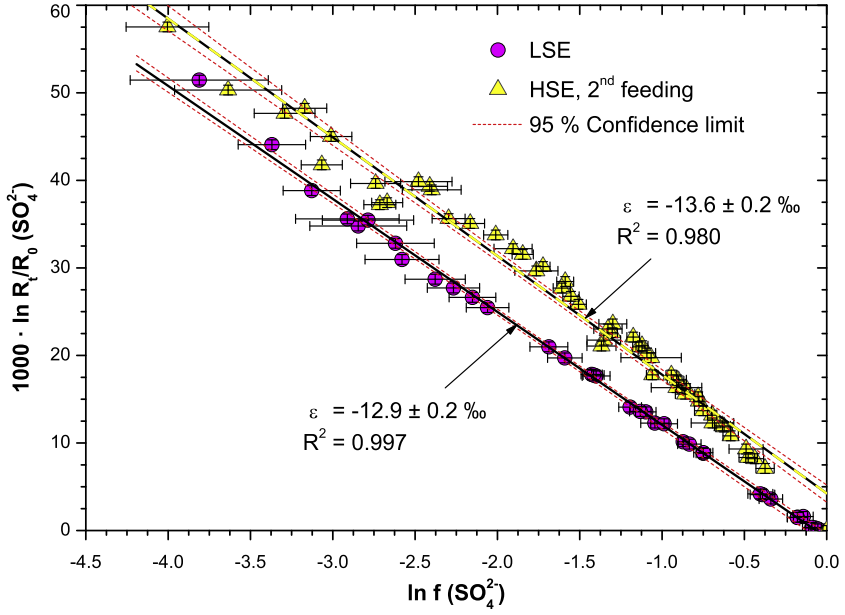

Fig. 7. Determination of the enrichment factors (ε) for the low sulfide (LSE, circles) and the high sulfide (HSE, triangles) experiment as the slope of a Rayleigh model fit according to Mariotti et al. (1981). R_t/R_0 are the isotope ratios of SO_4^{2-} at time t and $f(SO_4^{2-})$ represents the sulfate fraction remaining. Error bars are based on error propagations using single standard deviations. Regressions were not forced through zero following Scott et al. (2004).

i.e., ln (R_t/R_0) vs. ln $f(SO_4^{2-})_t$, as shown in Fig. 7 (according to Mariotti et al., 1981; Scott et al., 2004), we are only able to match the LSE data. The latter becomes evident in Fig. 8, where there is a large offset between HSE data and the trend line calculated from the Rayleigh enrichment factor of $-13.6 \pm 0.2‰$ for the HSE from Fig. 7. Since we know from Figs 7 and 8 that a Rayleigh fractionation model, which is directly derived from the HSE results, cannot explain the data, as an alternative, we tried to model the HSE data with a Rayleigh fractionation model using an enrichment factor that we manually adjusted by minimizing the RMSE and compared it with the results of the HSE. Fig. 9 compares four different Rayleigh fractionation curves based on the initial HSE conditions with our experimental

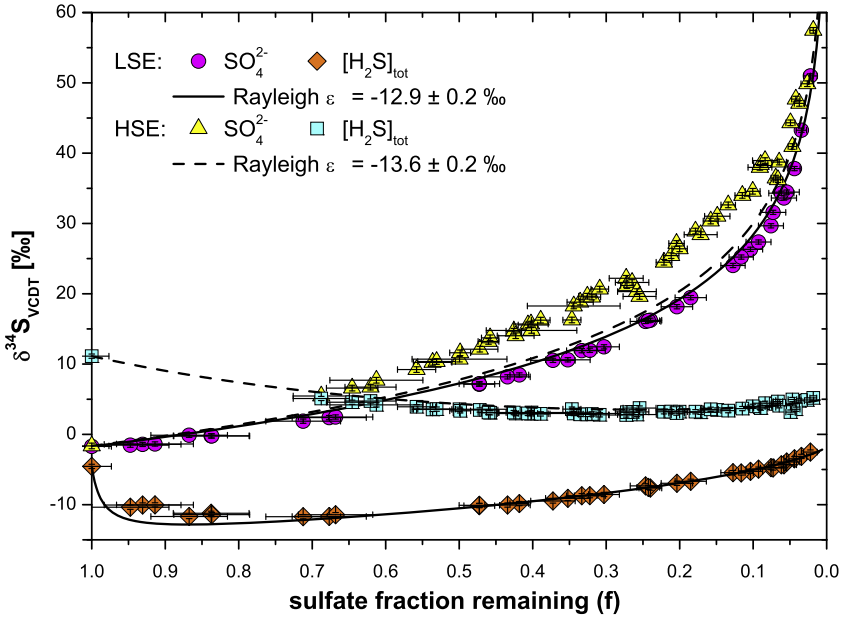

Fig. 8. Comparison of experimental S-isotope data with the corresponding Rayleigh model curves for sulfate and sulfide. The calculated enrichment factors for each experiment are estimated from Fig. 7: LSE: $\varepsilon = -12.9 \pm 0.2‰$ (solid lines) and HSE: $\varepsilon = -13.6 \pm 0.2‰$ (dashed lines). The more enriched $\delta^{34}S_{H_2S}$ starting point of $+11.1‰$ compared to the $-1.6‰$ of $\delta^{34}S_{SO_4^{2-}}$ during the HSE was generated by using enriched Na_2SO_4 for the first feeding cycle of the HSE (for more information see text).

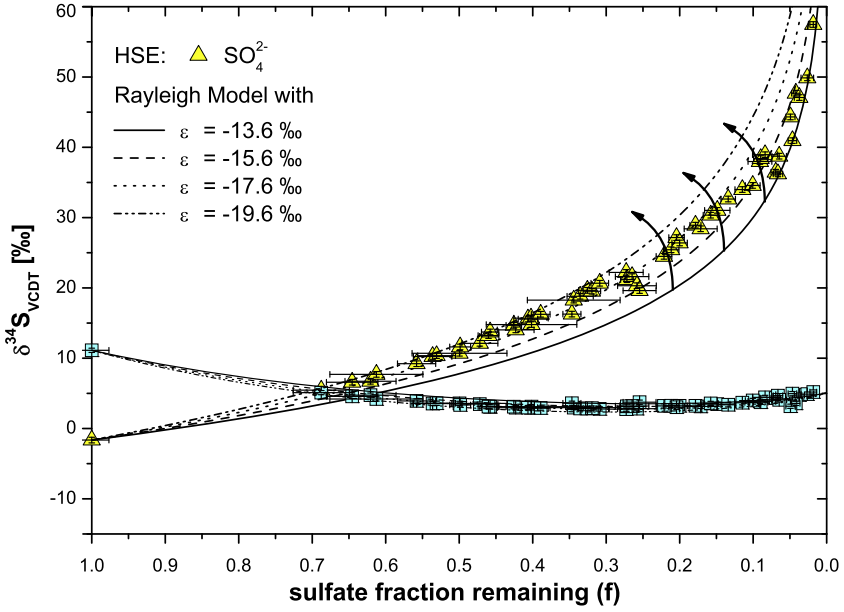

Fig. 9. Comparison between the second feeding of the HSE and four Rayleigh fractionation curves with different enrichment factors. The initial conditions are taken from the HSE and the calculations are based on Jørgensen (1979) and Mariotti et al. (1981). Arrows indicate the successive change with larger enrichments for the $\delta^{34}S$ of sulfate.

results. The lowest RMSE was found for $\varepsilon = -15.6‰$. From Fig. 9 it becomes evident that a 6‰ range in the enrichment factor, from $\varepsilon = -13.6$ to $-19.6‰$, would cover all experimental HSE results. But Fig. 9 also shows that none of the Rayleigh curves is able to match all HSE data at once (for $\varepsilon = -17.6‰$ see also Fig. 11). With more negative enrichment factors, the isotope data at low sulfate concentrations show an increasing offset to the Rayleigh model curve while the isotope data at medium sulfate concentrations show a decreasing offset. Neither the calculation of ε according to (Fig. 7, Mariotti et al., 1981) with an $\varepsilon = -13.6‰$ (solid line in Fig. 9) nor a regression line forced through zero, which yields $\varepsilon = -15.6‰$ (dashed line in Fig. 9) can match the HSE data satisfactory. Only when raising the enrichment factor to $\varepsilon = -17.6‰$, which increased the RMSE, the Rayleigh curve covers the HSE data in the medium sulfate concentration range down to $f = 0.13$ ($\ln f = -2.0$) but misses out in the low sulfate concentration range (dotted curve in Fig. 9 and dashed line in Fig. 11A). It could be argued that the sulfur isotope measurements were systematically underestimated for samples more enriched in $\delta^{34}S$ than +21‰, either because of a contamination with isotopically light sulfur impacting more strongly the measurements when sulfate becomes depleted, or due to non-linear behavior of the sulfur isotope measurements outside of the range covered by standards (i.e., NBS-127). However, we have no indication that either of these processes occurred, and there is no comparable pattern for the samples of the LSE, which should be the case for a systematic error.

In order to obtain a good match for the isotope data of the entire HSE, the isotope fractionation would have to be large (e.g., −17.6‰) at the start of the experiment and become much smaller towards the end (e.g., −13.6‰). However, this pattern is unlikely the result of a potential shift in growth phase, which we would expect to occur more likely at an early stage of the HSE (see Section D below). Under the assumption that all growth factors are the same for both experiments (see also text below), the pattern would rather have to be caused by a change in the ratio of the cell internal forward and backward fluxes induced by elevated sulfide concentrations. According to Brunner and Bernasconi (2005), this scenario appears to be unlikely too, because higher sulfide concentrations are expected to coincide with larger sulfur isotope fractionations, and because the isotope fractionation at low sulfate concentrations during the HSE should be similar to the one at low sulfate concentrations during the LSE. In contrast, our results indicate that the isotope fractionation requires to be highest at the start of the HSE. Therefore, changes in cell internal backward and forward flux ratios cannot be fully ruled out as an explanation for the observed non-Rayleigh isotope trends, but appear to be unlikely.

The differences in the $\delta^{34}S$-isotope trends between the calculated Rayleigh curves and the measured data for the HSE and LSE are more apparent for sulfate compared to sulfide (Fig. 8). The latter is a consequence of the fact that the $[H_2S]_{tot}$ pool represents an accumulated pool over time. Thus, isotopic changes in $\delta^{34}S_{H_2S}$ of any instantaneously produced H_2S have a less pronounced effect on the measured $\delta^{34}S_{H_2S}$ of the sulfide pool over time. However, we can estimate the enrichment of the instantaneously produced H_2S as the difference $\Delta^{34}S = \delta^{34}S_{H_2S} - \delta^{34}S_{SO_4^{2-}}$ between sulfate and the accumulated sulfide at the point of inflexion of the accumulated $\delta^{34}S_{H_2S}$ curve. The estimate for ε of the LSE is −12.5‰ (box with solid lines/arrow in Fig. 6), whereas the estimate of ε for the HSE ranged between −15.3‰ and −19.4‰ (boxes with dashed lines/arrows in Fig. 6). Both estimates reaffirmed the calculated enrichment factors with the Rayleigh fractionation model (Fig. 7) and point towards a non-Rayleigh type isotope fractionation behavior during the HSE. The latter could be caused by several processes: (A) Differences in the electron acceptor or substrate; (B) the formation and release of S-intermediates or cell external re-oxidation of sulfide to sulfate; (C) systematic errors in the S-isotope and/or sulfate concentration measurements; (D) changes in the growth behavior; (E) diffusion of sulfide back into the bacterial cell across the cell membrane, subsequent cell internal oxidation to sulfate, and transport of the newly formed sulfate back into the cell external sulfate pool.

(A) *Differences in the initial electron acceptor or substrate.* Based on the experimental batch culture setup, we assume that the re-feeding represented the only difference between the LSE and HSE, which resulted in a higher sulfide concentration in the HSE. The first feeding of the HSE used a Na_2SO_4, enriched in ^{34}S, as electron acceptor. X-ray fluorescence analysis of both batches of Na_2SO_4 did not reveal any significant variation in the elemental composition of the isotopically heavier and lighter Na_2SO_4. Thus, both batches of Na_2SO_4 should be interchangeable. In addition, we provided excess Na-acetate in both experiments to assure that the substrate is not a growth limiting factor in the LSE and HSE. Finally, a separate growth experiment using titanium citrate as the sole carbon source confirmed that *D. latus* does not grow on citrate as substrate, which we used as an initial reductant in all experiments. We therefore conclude that neither the substrate nor the electron donor caused the observed $\delta^{34}S_{SO_4^{2-}}$ offset in Fig. 6.

(B) *Formation and release of S-intermediates or cell external re-oxidation of sulfide to sulfate.* The observed S-isotope effect could have been a result of the formation and release of S-intermediates from the bacterial cell into the medium. However, our S-mass balance, which was solely based on the $[SO_4^{2-}]$ and $[H_2S]_{tot}$ concentration did not reveal any anomalies beyond the analytical error nor did we observe the development of a new peak on the ion chromatograph during SO_4^{2-} analysis that could have pointed towards the formation of S-intermediates. In general, the release of S-intermediates is rare and has only been observed in very few extreme cases, using cell extracts or conducting high temperature experiments (e.g., Fitz and Cypionka, 1990; Davidson et al., 2009). Thus, it is unlikely that the release of S-intermediates from the microorganism have caused the $\delta^{34}S_{SO_4^{2-}}$ offset during the second feeding of the HSE.

Another cause for the observed S-isotope effect in the sulfate pool could have been a result of cell external re-oxidation of sulfide to sulfate caused either by penetration of

oxygen through the butyl rubber septa or by oxidizing agents in the medium. The latter was excluded by equilibrium calculations with the geochemical model PHREEQC-2 (Parkhurst and Appelo, 1999) based on the chemical composition of the medium and the assumption of a stoichiometric reduction of sulfate and oxidation of acetate.

If an abiotic oxidation of sulfide had taken place, variations in the sulfide concentration of the three control bottles from the first feeding of the HSE would be expected since the bottles were only sampled and analyzed at the end of the HSE. The fact that no variation could be detected within error supports the notion that a cell external oxidation of sulfide by oxidizing agents in the medium, including dissolved oxygen, can be excluded.

(C) *Systematic errors in the S-isotope and/or sulfate concentration measurements.* If a systematic analytical error caused the observed S-isotopic offset between LSE and HSE, the error may have either solely occurred during the sample analysis of the HSE or been a result of a continuous $[H_2S]_{aq}$ re-oxidation that becomes more pronounced at higher $[H_2S]_{tot}$ levels. In the first case, it is unlikely that a systematic error occurred solely during the HSE given the fact that all experimental serum bottles were set up identically at the beginning of each experiment but chosen randomly for analysis at each individual time step. Furthermore, both S-isotope and sulfate concentration analyses of the HSE were handled identical to those of the LSE while none of the control vials showed an unexpected result with respect to sulfate S-isotopes and concentrations. The sulfate concentration in some of the experimental vials were measured twice, once immediately after sampling to monitor the overall degradation of sulfate and again once all the experimental samples were analyzed. Both independent sulfate concentration measurements exhibited identical results, which excludes time as cause for a systematic error. Although the second case, the one of a continuous $[H_2S]_{aq}$ re-oxidation that becomes more pronounced at higher $[H_2S]_{tot}$ levels, cannot be entirely excluded, the possibility of a re-oxidation of $[H_2S]_{aq}$ to sulfate is low based on the experimental setup and sample preparation (see Section 2).

(D) *Changes in growth behavior.* Both experiments, LSE and HSE, were incubated from a stock culture that was transferred at least three times from the main *D. latus* culture. Since the HSE was subject to two feeding cycles by adding only substrate and electron acceptor for the re-feeding, the measured isotope excursions could have been: (1) a result of vitamin or nutrient deficiencies, which affected the bacterial growth, or (2) a change in the growth phase as a result of two feeding cycles. Although there is no data support with respect to *D. latus* for those scenarios, we investigate in the following whether vitamin or nutrient deficiencies or a change in the growth behavior could have been responsible for the observed non-Rayleigh isotope trend during the HSE.

In addressing (1), *D. latus* requires only the vitamins thiamine and biotin as growth factors (Widdel, 1987, 1988). Considering that the largest amount of biomass produced during the HSE was $\approx$0.04 g DW L^{-1}, we provided 0.11% w/w of thiamine and 0.05% w/w biotin respectively of the produced biomass. In addition, the amount of provided macro- and microelements relative to the produced biomass remained in the range of required levels (Overmann, 2006). It is therefore unlikely that the media composition of the experiments caused the observed isotope trend.

With reference to (2), the cultures revealed exponential growth trends during the LSE and all feedings of the HSE but with an increased doubling time during the second feeding of the HSE by a factor of 3.6 compared to the LSE (Section 4.1 and Fig. 4). From a statistical point of view, the increase in doubling time during the second feeding of the HSE was not significant regarding the growth yield (Fig. 5). Nevertheless, as the potential increase in doubling time could reflect a change in the metabolic activity of our cultures, we explore this possibility here in more detail.

The increase in the doubling time during the HSE could be due to the delayed re-feeding with sulfate causing the cells to enter a stationary or decay phase. The cells could also require a higher maintenance energy during the HSE due to higher sulfide concentrations as suggested by Okabe et al. (1995). Our TCC data indicate a reduced TCC number at the beginning of the second feeding which could point to cell decay. Because the direct cell count method with DAPI does not allow discrimination between live and dead cells, we cannot fully explore the results in this respect. However, the actual biomass involved in decay processes is so small that there would be no measurable effect on the concentration or isotopic signature of the sulfate and sulfide pools in our experiments. Nonetheless, cultures in a stationary or decay phase are expected to fractionate isotopes differently than cultures during exponential growth (Davidson et al., 2009). Based on the findings of Fukui et al. (1996), who described a high survival efficiency of *D. latus* with the capability of keeping high levels of rRNA under starvation, we assume for the HSE that the culture regained efficient growth almost immediately after re-feeding with sulfate. This notion is supported by the lack of a pronounced lag phase during the HSE.

As a result of the aforementioned discussion on variations in the growth phase, it cannot be ruled out that the cultures were in a stationary or decay phase at the start of the HSE, but if so, it is likely that the cultures regained exponential growth rapidly after starting the HSE. Thus, one would expect that the sulfur isotope fractionation may have changed in an early stage of the HSE when the cultures switched from stationary to exponential growth phase, but with no further change in the isotope fractionation during the exponential growth phase. Therefore, we would still expect to see a Rayleigh type fractionation behavior during most of the HSE experiment. In addition, we also modeled a hypothetical Rayleigh scenario, in which we assumed a changing enrichment factor during exponential growth (data not shown). Although it was possible in such a scenario to match the data with a decreasing enrichment factor, the result implies that high sulfide levels induce smaller isotope fractionations and there is currently no mechanistic model on an enzymatic level that would explain

such a change in the enrichment factor over time. Consequently, we consider the possibility that changes in growth behavior caused the observed non-Rayleigh behavior during the HSE as minor.

(E) *Diffusion of sulfide back into the bacterial cell across the cell membrane, and subsequent re-oxidation to sulfate.* To investigate this scenario, we use a model, which allows for a Rayleigh type fractionation during sulfate reduction and a non-fractionating backward flow (see model development). The backward flow b_2 (Fig. 3) is governed by a 1st order kinetic term that depends on the cell external concentration of dissolved $[H_2S]_{aq}$, which varies as a function of pH. Fig. 10 illustrates the evolution and slight increase of the pH (dotted line) over the course of two feedings in comparison to the increase of undissociated dissolved $[H_2S]_{aq}$ (solid line), dissociated $[HS^-]$ (dashed line), and the sum of both ($[H_2S]_{tot}$, dashed dotted line) during the same feeding period. As a result of the increasing $[H_2S]_{tot}$, the undissociated $[H_2S]_{aq}$ continuously increases over the course of the experiment. Fig. 10 demonstrates that a slight increase of the pH, which shifts the $[H_2S]_{aq}/[HS^-]$ equilibrium towards dissociated $[HS^-]$, does not fully eliminate the increase in undissociated $[H_2S]_{aq}$. By the end of the HSE, $[H_2S]_{aq}$ still comprises 30% of the $[H_2S]_{tot}$ pool. Since undissociated $[H_2S]_{aq}$ is assumed to freely diffuse through the bacterial cell membrane (Cypionka, 1987, 1989, 1995; Bagarinao, 1992), we assume that $[H_2S]_{aq}$ triggers a backward flow of hydrogen sulfide in our SRF reflux model. In an experimental study, Moosa and Harrison (2006) support the notion that undissociated $[H_2S]_{aq}$ functions as an active agent. Although we cannot completely exclude an active transport system that moves dissociated $[HS^-]$ across the cytoplasmic membrane (e.g., driven by sodium ions), we did not find any evidence for such a system in the literature with respect to bisulfide.

In our model, we fitted the 1st order rate constant (k_{re}), which defines the extend of the $[H_2S]_{aq}$ backward flow, simultaneously with the initial enrichment factor $\varepsilon_a(t=0)$ by minimizing the RMSE between experimental and model results (see model development). We can estimate k_{re} and $\varepsilon_a(t=0)$ by matching the output of our SRF reflux model to the data (Fig. 11A). The estimated values for $\varepsilon_a(t=0) = -11.1‰$ and $k_{re} = 1.0 \times 10^{-16}$ L cell^{-1} s^{-1} are derived for both independent data sets. The modeling was conducted with a ε_a(tot) of $-70‰$ (Brunner and Bernasconi, 2005), and an estimated average cell specific sulfate reduction rate (csSRR) of 860 fmol SO_4^{2-} cell^{-1} d^{-1}, which is comparable with a csSRR of 1050 fmol SO_4^{2-} cell^{-1} d^{-1} of the mesophilic *Desulfobacter curvatus* strain '*ak30*' (Isaksen and Jørgensen, 1996).

Unlike a unidirectional Raleigh type fractionation, which results in two slightly different enrichment factors for each experiment that cannot account for the $\delta^{34}S_{SO_4^{2-}}$ offset between LSE and HSE (Fig. 8), our sulfide reflux model reproduces the isotopic offset between the two experiments using a single set of boundary conditions (Fig. 11A and B). The result of our model implies that the diffusive transport across the cell membrane is bi-directional and sulfide can be re-oxidized to sulfate during ongoing sulfate reduction. This finding strongly supports the hypothesis that the entire chain of enzymatic reactions controlling DSR is reversible (Brunner and Bernasconi, 2005) and that the reversibility depends on the cell external sulfide concentration. Our interpretation is supported by the thermodynamic concept for a reversible enzymatic process: The closer such an enzymatic process is to the thermodynamic equilibrium the more reversible the process becomes (Moore and Pearson, 1981; Morgan and Stone, 1985). Furthermore, the overall reversibility of an enzymatic process does not change if more enzymatic steps are introduced into the reaction chain, because the overall energy yield is distributed over a larger number of steps in such a scenario.

Based on our model and by integrating all $[H_2S]_{aq}$ refluxes ($b_2(t)$ in Fig. 3) over time for both experiments, we calculate that during the LSE and HSE a total of 4% and 10%, respectively of the sulfide-S were recycled and re-oxidized to sulfate during DSR.

Our results pose however an interesting challenge. The observed Rayleigh enrichment factors of $-12.9‰$ and $-13.6‰$ are approximately half of the isotope enrichment factor commonly attributed to the reduction of APS to sul-

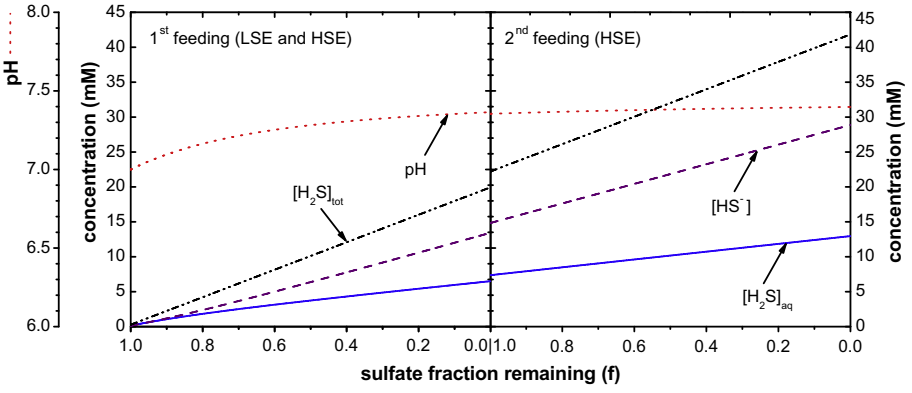

Fig. 10. Evolution of pH (dotted line), total dissolved sulfide $[H_2S]_{tot} = [H_2S]_{aq} + [HS^-]$ (dashed dotted line), dissociated $[HS^-]$ (dashed line), and undissociated $[H_2S]_{aq}$ (solid line) over the course of the re-feeding experiment. The concentration curves are based on equilibrium calculations with the geochemical model PHREEQC-2 (Parkhurst and Appelo, 1999). The *x*-axis shows the fraction of remaining sulfate (*f*) during sulfate reduction for both feedings.

fite (−25‰ for step III in Fig. 1, Rees, 1973), implying that APS reduction could be the rate limiting step. For the traditional model, the same would be true if the reduction of sulfite and not APS is rate limiting with an associated $\varepsilon = -25‰$ (Rees, 1973) for the sulfite reduction step. Regardless which one of the two steps is rate limiting, the traditional notion (e.g., Rees, 1973) holds that in case of a rate limiting step, there are no backward fluxes associated with downstream reduction steps. However, our results indicate that backward fluxes occur downstream of the APS reduction step (Fig. 1). Thus, in the light of our HSE experiment and model calculation, which suggests an existing S-reflux through the whole reduction chain of Fig. 1, including the rate limiting step, we prefer to use the expression "bottleneck" rather than "rate limiting" for the step in the sulfate reduction chain that triggers the observed isotope enrichment. For us, the term bottleneck simply implies that forward and backward fluxes may coexist for a particular fractionating step, as suggested in Fig. 1. In our simplified single step fractionation model, these forward and backward fluxes are expected to affect the overall enrichment factor, i.e., the enrichment factor should get larger. It is beyond the scope of this paper to explore the isotope effects for a multi-step sulfate reduction network in detail. However, we observe that the introduction of a $[H_2S]_{aq}$ dependent backward flux in our simplified sulfate reduction and fractionation model – i.e., the backward flux is based on a 1st order kinetic, no internal mixing, and using the maximum enrichment factor published by Brunner and Bernasconi (2005) – results in overall fractionation factors that are consistent with our measurements. Abandoning the idea that the overall fractionation factor is con-

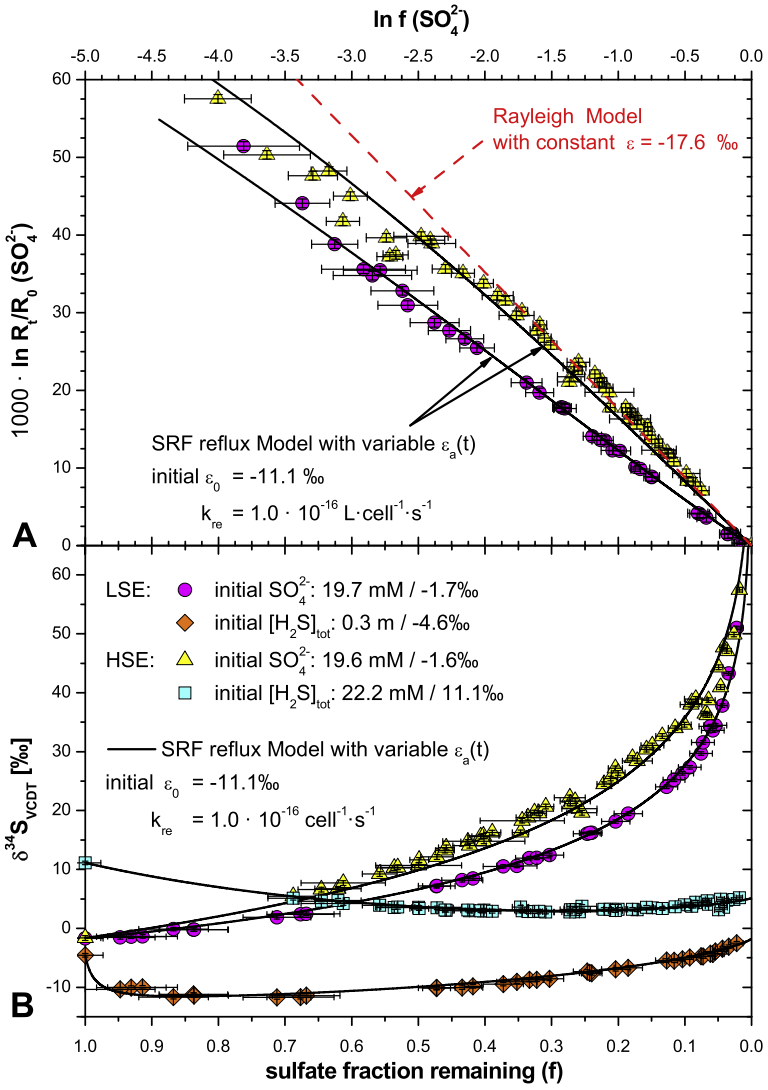

Fig. 11. SRF model curve with sulfide reflux (solid lines) including both LSE and HSE data (LSE: circles (SO_4^{2-}), diamonds ($[H_2S]_{tot}$) and HSE: triangles (SO_4^{2-}), squares ($[H_2S]_{tot}$)). (A) Both SRF curves are modeled simultaneously using the same initial ε_0 and k_{re} value but allowing for a variable enrichment factor $\varepsilon_a(t)$ over time. In comparison, the dashed line outlines a Rayleigh model curve for the HSE with a constant $\varepsilon = -17.6‰$ (cf. Fig. 9). (B) SRF reflux model (solid lines) in $\delta^{34}S$ vs. $f(SO_4^{2-})$ space. Unlike the Rayleigh model in (A) or Fig. 8, the SRF reflux model is able to simulate simultaneously the results of both LSE and HSE.

trolled by a single rate limiting step also resolves the apparent contradiction with the hypothesis that reversibility of sulfate reduction induced by high sulfide concentrations would result in extremely high fractionation factors (Brunner and Bernasconi, 2005).

5. CONCLUSIONS

While the reversibility of the individual enzymatic steps during microbially mediated sulfate reduction has been recognized long ago, only a few studies explored the actual process. It is clear however, that at least the steps leading to the intermediate sulfite (first three steps in Fig. 1) must be reversible (Farquhar et al., 2003; Brunner and Bernasconi, 2005; Johnston et al., 2005, 2007; Canfield et al., 2006; Wortmann et al., 2007), and that the oxygen isotope exchange flux via intermediates (b_1, b_2, and probably b_3, Fig. 1) can exceed the net-reduction flux (f_3, Fig. 1) by at least an order of magnitude (Wortmann et al., 2007), while up to 96% of sulfate can be recycled to the medium (b_1, Fig. 1, according to Farquhar et al., 2008). Still, much less is known about the reversibility of the reduction of sulfite to H_2S (step IV, Fig. 1) and the transport of H_2S across the cell membrane (step V, Fig. 1). Farquhar et al. (2008) indicate that there might be a reversibility downstream of sulfite in step IV (Fig. 1) during DSR, which supports the conceptual model of Brunner and Bernasconi (2005). In addition, Moosa and Harrison (2006) argue that undissociated $[H_2S]_{aq}$ rather than $[H_2S]_{tot}$ influences the volumetric sulfate reduction rate, which can be seen as an indicator for a potential reversibility in step V (Fig. 1).

Our findings demonstrate that sulfate reduction by *D. latus* under high ambient sulfide concentrations (>22 mM) results in a non-Rayleigh type fractionation behavior, which is consistent with a model that allows for the cell internal re-oxidation of sulfide to sulfate. From a modeling perspective, we cannot distinguish between cell-internal and cell-external oxidation, however the experimental setup precludes the latter. We therefore propose for *D. latus* that sulfide is transported backwards across the cytoplasmic membrane during DSR, is subsequently re-oxidized to sulfate, and returned to the cell external sulfate pool. Our results strongly support the findings of Trudinger and Chambers (1973) who used ^{35}S-labeled H_2S in a study with *Desulfovibrio desulfuricans* and discovered the formation of ^{35}S-labeled sulfate during sulfate reduction suggesting reversible, cell internal enzymatic pathways during DSR.

Our findings hint at the possibility that the traditional notion of a rate limiting step (e.g., Rees, 1973) may better be expressed as a bottleneck to clarify the potential coexistence of forward and backward fluxes. It may also have to be expanded in favor of a model that involves the entire enzymatic reaction chain. Our results are however not detailed enough to explore this possibility more comprehensively.

ACKNOWLEDGMENTS

TE would like to thank The Agouron Institute and the USC Wrigley Institute who made him, the analytical geochemist, acquainted with applied microbial techniques during the Geobiology Course 2005. The work was conducted in cooperation with the Department of Chemical Engineering and Applied Chemistry at the University of Toronto. In particular, TE likes to thank Martin Elsner and Volker Brüchert for their input and discussions on the Rayleigh fractionation and the microbial setup at the early stages of the project and Georges Lacrampe Couloume, Hong Li, and Nicole DeBond for their help with experimental design, sample analysis and cheerful spirits. This project was supported by a NSERC discovery grant to UGW. We also thank David Johnston and two anonymous reviewers for their thorough revisions and constructive comments as well as AE Timothy W Lyons.

REFERENCES

Bagarinao T. (1992) Sulfide as an environmental factor and toxicant: tolerance and adaptations in aquatic organisms. *Aquat. Toxicol.* **24**(1–2), 21–62.

Bakken L. R. and Olsen R. A. (1983) Buoyant densities and dry-matter contents of microorganisms: conversion of a measured biovolume into biomass. *Appl. Microbiol. Biotechnol.* **45**(4), 1188–1195.

Berner R. A. (1970) Sedimentary pyrite formation. *Am. J. Sci.* **268**, 1–23.

Berner R. A. (1984) Sedimentary pyrite formation: an update. *Geochim. Cosmochim. Acta* **248**, 605–615.

Bolliger C., Schroth M. H., Bernasconi S. M., Kleikemper J. and Zeyer J. (2001) Sulfur isotope fractionation during microbial sulfate reduction by toluene-degrading bacteria. *Geochim. Cosmochim. Acta* **65**(19), 3289–3298.

Brunner B. and Bernasconi S. M. (2005) A revised isotope fractionation model for dissimilatory sulfate reduction in sulfate reducing bacteria. *Geochim. Cosmochim. Acta* **69**(20), 4759–4771.

Brunner B., Bernasconi S. M., Kleikemper J. and Schroth M. H. (2005) A model for oxygen and sulfur isotope fractionation in sulfate during bacterial sulfate reduction processes. *Geochim. Cosmochim.* **69**(20), 4773–4785.

Canfield D. E. (2001) Isotope fractionation by natural populations of sulfate-reducing bacteria. *Geochim. Cosmochim. Acta* **65**(7), 1117–1124.

Canfield D. E., Farquhar J. and Zerkle A. L. (2010) High isotope fractionations during sulfate reduction in a low-sulfate euxinic ocean analog. *Geology* **38**(5), 415–418.

Canfield D. E., Olesen C. A. and Cox R. P. (2006) Temperature and its control of isotope fractionation by a sulfate-reducing bacterium. *Geochim. Cosmochim. Acta* **70**(3), 548–561.

Canfield D. E. and Teske A. (1996) Late proterozoic rise in atmospheric oxygen concentration inferred from phylogenetic and sulphur-isotope studies. *Nature* **382**(6587), 127–132.

Canfield D. E. and Thamdrup B. (1994) The production of S^{34}-depleted sulfide during bacterial disproportionation of elemental sulfur. *Science* **266**(5193), 1973–1975.

CIAAW (2007) Sulfur isotopic reference – $\delta^{34}S$ values of sulfur isotopic reference materials. Technical Report, Commission on Isotopic Abundances and Atomic Weights, URL: http://www.ciaaw.org/sulfur.htm.

Cline J. D. (1969) Spectrophotometric determination of hydrogen sulfide in natural waters. *Limnol. Oceanogr.* **14**(3), 454–458.

Cypionka H. (1987) Uptake of sulfate, sulfite and thiosulfate by proton-anion symport in Desulfovibrio desulfuricans. *Arch. Microbiol.* **148**(2), 144–149.

Cypionka H. (1989) Characterization of sulfate transport in *Desulfovibrio desulfuricans*. *Arch. Microbiol.* **152**(3), 237–243.

Cypionka H. (1995) Solute transport and cell energetics. In *Sulfate-Reducing Bacteria* (ed. L.L. Barton). Plenum Press, New York, Biotechnology Handbooks, vol. **8**. pp. 151–184.

Cypionka H., Smock A. M. and Böttcher M. E. (1998) A combined pathway of sulfur compound disproportionation in *Desulfovibrio desulfuricans*. *Microbiol. Lett.* **166**(2), 181–186.

Davidson M. M., Bisher M. E., Pratt L. M., Fong J., Southam G., Pfiffner S. M., Reches Z. and Onstott T. C. (2009) Sulfur isotope enrichment during maintenance metabolism in the thermophilic sulfate-reducing bacterium desulfotomaculum putei. *Appl. Microbiol. Biotechnol.* **75**(17), 5621–5630.

Detmers J., Brnchert V., Habicht K. S. and Kuever J. (2001) Diversity of sulfur isotope fractionations by sulfate-reducing prokaryotes. *Appl. Microbiol. Biotechnol.* **67**(2), 888–894.

Farquhar J., Canfield D. E., Masterson A., Bao H. and Johnston D. (2008) Sulfur and oxygen isotope study of sulfate reduction in experiments with natural populations from Fællestrand, Denmark. *Geochim. Cosmochim. Acta* **72**(12), 2805–2821.

Farquhar J., Johnston D. T., Wing B. A., Habicht K. S., Canfield D. E., Airieau S. and Thiemens M. H. (2003) Multiple sulphur isotopic interpretations of biosynthetic pathways: implications for biological signatures in the sulphur isotope record. *Geobiology* **1**(1), 27–36.

Ferenci T. (1999) 'Growth of bacterial cultures' 50 years on: towards an uncertainty principle instead of constants in bacterial growth kinetics. *Res. Microbiol.* **150**(7), 431–438.

Fishman M. J. and Friedman L. C. (1989) Techniques of water-resources investigations of the united states geological survey. *Laboratory Analysis: Methods for Determination of Inorganic Substances in Water and Fluvial Sediments TWRI5-A1*. US Geological Survey, Reston, VA, USA.

Fitz R. M. and Cypionka H. (1990) Formation of thiosulfate and trithionate during sulfite reduction by washed cells of desulfovibrio–desulfuricans. *Arch. Microbiol.* **154**(4), 400–406.

Fry J. C. (1988) Determination of biomass. In *Methods in Aquatic Bacteriology, Modern Microbiological Methods* (ed. B. Austin). Wiley, New York, pp. 27–72 (Chapter 2).

Fukui M., Suwa Y. and Urushigawa Y. (1996) High survival efficiency and ribosomal rna decaying pattern of *Desulfobacter latus*, a highly specific acetate-utilizing organism, during starvation. *FEMS Microbiol. Ecol.* **19**(1), 17–25.

Funk W., Dammann V. and Donnevert G. (2007) *Quality Assurance in Analytical Chemistry*, second ed. Wiley-VCH Verlag, Weinheim.

Habicht K. S., Salling L., Thamdrup B. and Canfield D. E. (2005) Effect of low sulfate concentrations on lactate oxidation and isotope fractionation during sulfate reduction by *Archaeoglobus fulgidus* Strain Z. *Appl. Microbiol. Biotechnol.* **71**(7), 3770–3777.

Hadas O., Malinsky-Rushansky N., Pinkas R. and Cappenberg T. E. (1998) Grazing on autotrophic and heterotrophic picoplankton by ciliates isolated from Lake Kinneret, Israel. *J. Plankton. Res.* **20**(8), 1435–1448.

Harrison A. G. and Thode H. G. (1958) Mechanism of the bacterial reduction of sulphate from isotope fractionation studies. *Trans. Faraday Soc.* **54**(1), 84–92.

Hoek J., Reysenbach A. L., Habicht K. S. and Canfield D. E. (2006) Effect of hydrogen limitation and temperature on the fractionation of sulfur isotopes by a deep-sea hydrothermal vent sulfate-reducing bacterium. *Geochim. Cosmochim. Acta* **70**(23), 5831–5841.

Hyun J. H. and Yang E. J. (2003) Freezing seawater for the long-term storage of bacterial cells for microscopic enumeration. *J. Microbiol.* **41**(3), 262–265.

Icgen B. and Harrison S. (2006) Exposure to sulfide causes populations shifts in sulfate-reducing consortia. *Res. Microbiol.* **157**(8), 784–791.

Isaksen M. F. and Jørgensen B. B. (1996) Adaptation of psychrophilic and psychrotrophic sulfate-reducing bacteria to permanently cold marine environments. *Appl. Microbiol. Biotechnol.* **62**(2), 408–414.

Morgan J. J. and Stone A. T. (1985) Kinetics of chemical processes of importance in lacustrine environments. In *Chemical Processes in Lakes* (ed. W. Stumm). Wiley, New York. pp. 389–426 (Chapter 17).

Moore J. W. and Pearson R. G. (1981) *Kinetics and Mechanism*, third ed. Wiley, New York.

Johnston D. T., Farquhar J. and Canfield D. E. (2007) Sulfur isotope insights into microbial sulfate reduction: when microbes meet models. *Geochim. Cosmochim. Acta* **71**(16), 3929–3947.

Johnston D. T., Farquhar J., Wing B. A., Kaufman A., Canfield D. E. and Habicht K. S. (2005) Multiple sulfur isotope fractionations in biological systems: a case study with sulfate reducers and sulfur disproportionators. *Am. J. Sci.* **305**(6–8), 645–660.

Jones G. A. and Pickard M. D. (1980) Effect of titanium(III) citrate as reducing agent on growth of rumen bacteria. *Appl. Microbiol. Biotechnol.* **39**(6), 1144–1147.

Jørgensen B. B. (1979) A theoretical model of the stable sulfur isotope distribution in marine sediments. *Geochim. Cosmochim. Acta* **43**(3), 363–374.

Jørgensen B. B. (2006) Bacteria and marine biogeochemistry. In *Marine Geochemistry* (eds. H. D. Schulz and M. Zabel). Springer, Berlin, pp. 169–206 (Chapter 5).

Jørgensen B. B., Böttcher M. E., Luschen H., Neretin L. N. and Volkov I. (2004) Anaerobic methane oxidation and a deep H_2S sink generate isotopically heavy sulfides in black sea sediments. *Geochim. Cosmochim. Acta* **68**(9), 2095–2118.

Kaplan I. R. and Rittenberg S. C. (1964) Microbiological fractionation of sulphur isotopes. *J. Gen. Microbiol.* **34**(2), 195–212.

Kemp A. L. W. and Thode H. G. (1968) The mechanism of bacterial reduction of sulphate and of sulphite from isotope fractionation studies. *Geochim. Cosmochim. Acta* **32**(1), 71–91.

Kinoshita M. and Paynter M. J. B. (1988) A self-refilling syringe for dispensing anaerobic media. *Biotechnol. Tech.* **2**(3), 159–162.

Knoblauch C. and Jørgensen B. B. (1999) Effect of temperature on sulphate reduction, growth rate and growth yield in five psychrophilic sulphate-reducing bacteria from arctic sediments. *Environ. Microbiol.* **1**(5), 457–467.

Lide, D. R. (ed.) (2006) *CRC Handbook of Chemistry and Physics: A Ready-reference Book of Chemical and Physical Data*, 87th ed. Taylor and Francis, New York.

Lloyd K. G., Edgcomb V. P., Molyneaux S. J., Boer S., Wirsen C. O., Atkins M. S. and Teske A. (2005) Effects of dissolved sulfide, ph, and temperature on growth and survival of marine hyperthermophilic archaea. *Appl. Environ. Microbiol.* **71**(10), 6383–6387.

Madigan M. T. (2006) *Brock Biology of Microorganisms*, 11th ed. Pearson Prentice Hall, Upper Saddle River, NJ.

Mangalo M., Einsiedl F., Meckenstock R. U. and Stichler W. (2008) Influence of the enzyme dissimilatory sulfite reductase on stable isotope fractionation during sulfate reduction. *Geochim. Cosmochim. Acta* **72**(6), 1513–1520.

Mangalo M., Meckenstock R. U., Stichler W. and Einsiedl F. (2007) Stable isotope fractionation during bacterial sulfate reduction is controlled by reoxidation of intermediates. *Geochim. Cosmochim. Acta* **71**(17), 4161–4171.

Mariotti A., Germon J. C., Hubert P., Kaiser P., Letolle R., Tardieux A. and Tardieux P. (1981) Experimental-determination of nitrogen kinetic isotope fractionation – some principles – illustration for the denitrification and nitrification processes. *Plant Soil* **62**(3), 413–430.

Mayer B. and Krouse H. R. (2004) Procedures for sulfur isotope abundance studies. In *Handbook of stable isotope analytical techniques*, vol. 1 (ed. P. A. de Groot). Elsevier, Amsterdam, pp. 538–603 (Chapter 26).

Moosa S. and Harrison S. T. L. (2006) Product inhibition by sulphide species on biological sulphate reduction for the treatment of acid mine drainage. *Hydromet* **83**(1–4), 214–222.

Okabe S., Nielsen P. H. and Characklis W. G. (1992) Factors affecting microbial sulfate reduction by *Desulfovibrio desulfuricans* in continuous culture – limiting nutrients and sulfide concentration. *Biotechnol. Bioeng.* **40**(6), 725–734.

Okabe S., Nielsen P. H., Jones W. L. and Characklis W. G. (1995) Sulfide product inhibition of *Desulfovibrio desulfuricans* in batch and continuous cultures. *Water Res.* **29**(2), 571–578.

Overmann J. (2006) Principles of enrichment, isolation, cultivation and preservation of prokaryotes. In *The Prokaryotes*, vol. 1 (eds. M. Dworkin, S. Falkow, E. Rosenberg, K. H. Schleifer and E. Stackebrandt). Springer, New York, pp. 80–136 (third ed., Chapter 1.5).

Parkhurst D. L. and Appelo C. A. J. (1999) User's guide to PHREEQC (version 2); a computer program for speciation, batch-reaction, one-dimensional transport, and inverse geochemical calculations. *Water-Resources Investigations Report 99-4259*. US Geological Survey, Reston, VA, USA.

Postgate J. R. (1984) *The Sulphate-Reducing Bacteria*, second ed. Cambridge Univ. Press, Cambridge.

Rees C. E. (1973) Steady-state model for sulfur isotope fractionation in bacterial reduction processes. *Geochim. Cosmochim. Acta* **37**(5), 1141–1162.

Robinson J. A. and Tiedje J. M. (1983) Non-linear estimation of monod growth kinetic-parameters from a single substrate depletion curve. *Appl. Microbiol. Biotechnol.* **45**(5), 1453–1458.

Rudnicki M. D., Elderfield H. and Spiro B. (2001) Fractionation of sulfur isotopes during bacterial sulfate reduction in deep ocean sediments at elevated temperatures. *Geochim. Cosmochim. Acta* **65**(5), 777–789.

Scott K. M., Lu X., Cavanaugh C. M. and Liu J. S. (2004) Optimal methods for estimating kinetic isotope effects from different forms of the Rayleigh distillation equation. *Geochim. Cosmochim. Acta* **68**(3), 433–442.

Szabo A., Tudge A., Macnamara J. and Thode H. G. (1950) The distribution of S-34 in nature and the sulfur cycle. *Science* **111**(2887), 464–465.

Thode H. G., Kleerekoper H. and McElcheran D. (1951) Isotope fractionation in the bacterial reduction of sulfate. *Res. Lond.* **4**, 581–582.

Trudinger P. A. and Chambers L. A. (1973) Reversibility of bacterial sulfate reduction and its relevance to isotope fractionation. *Geochim. Cosmochim. Acta* **37**(7), 1775–1778.

Werne J. P., Lyons T. W., Hollander D. J., Formolo M. J. and Damste J. S. S. (2003) Reduced sulfur in euxinic sediments of the Cariaco Basin: sulfur isotope constraints on organic sulfur formation. *Chem. Geol.* **195**(1–4), 159–179.

Widdel F. (1987) New types of acetate-oxidizing, sulfate-reducing *Desulfobacter* species, *D. hydrogenophilus* sp. nov., *D. latus* sp. nov., and *D. curvatus* sp. nov.. *Arch. Microbiol.* **148**(4), 286–291.

Widdel F. (1988) *Microbiology and Ecology of Sulfate- and Sulfur-Reducing Bacteria, Ecological and Applied Microbiology*. Wiley, New York (Chapter 10, pp. 469–585).

Widdel F. and Bak F. (1992) Gram-negative mesophilic sulfate-reducing bacteria. In *The Prokaryotes* (eds. A. Balows, H. G. Trueper, M. Dworkin, W. Harder and K. H. Schleifer). Springer, New York, vol. **4**. pp. 3352–3378 (2nd ed.).

Wortmann U. G., Bernasconi S. M. and Böttcher M. E. (2001) Hypersulfidic deep biosphere indicates extreme sulfur isotope fractionation during single-step microbial sulfate reduction. *Geology* **29**(7), 647–650.

Wortmann U. G., Chernyavsky B., Bernasconi S. M., Brunner B., Böttcher M. E. and Swart P. K. (2007) Oxygen isotope biogeochemistry of pore water sulfate in the deep biosphere: dominance of isotope exchange reactions with ambient water during microbial sulfate reduction (ODP Site 1130). *Geochim. Cosmochim. Acta* **71**(17), 4221–4232.

Wortmann U. G. and Chernyavsky B. M. (2007) Effect of evaporite deposition on Early Cretaceous carbon and sulphur cycling. *Nature* **446**(7136), 654–656.

Zehnder A. J. B. and Wuhrmann K. (1976) Titanium (III) citrate as a nontoxic oxidation-reduction buffering system for culture of obligate anaerobes. *Science* **194**(4270), 1165–1166.

Associate editor: Timothy W. Lyons